

Photochemical Synthesis and Electronic Properties of Extended Corannulenes with Variable Fluorination Pattern

Dzeneta Halilovic,[†] Maja Budanović,[†] Zeng R. Wong,[†] Richard D. Webster,[†] June Huh,^{*,‡} and Mihaiela C. Stuparu^{*,†,§}

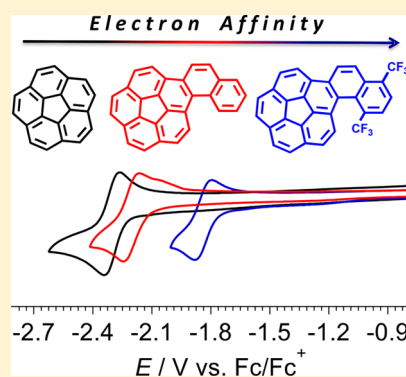
[†]Division of Chemistry and Biological Chemistry, School of Physical and Mathematical Sciences, Nanyang Technological University, 21-Nanyang Link, 637371, Singapore

[‡]Department of Chemical and Biological Engineering, Korea University, Seoul 02841, Korea

[§]School of Materials Science and Engineering, Nanyang Technological University, 50 Nanyang Avenue, 639798, Singapore

Supporting Information

ABSTRACT: The first family of extended and fluorinated corannulenes is prepared through a highly efficient and modular synthetic strategy. In this strategy, corannulene aldehyde could be combined with the fluorine-carrying phosphonium ylides to furnish stilbene-like vinylene precursors. A photochemically induced oxidative cyclization process of these precursors gives rise to the fluorinated and curved polycyclic aromatic hydrocarbons. A UV–vis absorption study shows that aromatic extension results in a bathochromic shift of about 12 nm. Fluorination further shifts the absorption spectrum to the red region, and a maximum shift of about 22 nm is detected for a compound carrying two trifluoromethyl groups. A cyclic and square-wave voltammetry investigation reveals that the extension of the corannulene scaffold increases the reduction potential by 0.11 V. Placement of fluorine or trifluoromethyl groups further enhances the electron affinities. In this regard, the presence of one trifluoromethyl group equals the effect of three aromatic fluorine atoms. Molecules with two trifluoromethyl groups, meanwhile, exhibit the highest reduction potentials of -1.93 and -1.83 V. These values are 0.37 and 0.46 V higher than those of the parental corannulene and demonstrate the utility of the present design concept by efficiently accessing effective electron acceptors based on the buckyball motif.



INTRODUCTION

Fluorinated corannulene derivatives have been known to be good electron acceptors.^{1–6} This property, therefore, suggests potential applications in the vast arena of organic electronics. In this context, in 2012, Boltalina and co-workers showed that a gas phase synthesis could be employed for the introduction of five trifluoromethyl groups onto the corannulene scaffold.¹ However, harsh reaction conditions and a tedious purification procedure coupled with a low yield of the final compound (15%) restrict wide applicability of such a synthetic protocol. In the same year, the group of Lentz reported the synthesis of corannulene carrying one, two, and three trifluoromethyl groups at predefined positions on the corannulene nucleus.² In this case, the synthesis was in a solution phase and more practical albeit still suffering from low overall yields. Very recently, Baldrige and Siegel have shown that readily available halocorannulene and corannuleneboronates can undergo copper-mediated Hartwig/Yagupolskii coupling processes to yield a variety of fluorinated corannulenes in moderate to good yields (up to 80% in some cases).⁵ A systematic structure–property relationship development also suggested that each trifluoromethyl group shifted the first reduction potential of the corannulene nucleus by 0.22 V. Direct placement of electron withdrawing substituents, such as the trifluoromethyl groups,

thus, is an established route to modulate the electronic properties of the bowl-shaped aromatic nucleus.⁶

An alternative strategy to meet this goal is through extending the aromatic area of the corannulene scaffold by annulation to planar π -systems that are polycyclic. Siegel and co-workers have established that such aromatic framework extensions can allow for the variation of such electronic properties.⁷ The final molecules in this approach can be imagined as hybrids of planar and nonplanar aromatic structures and are referred to as “extended corannulenes”. Besides Siegel’s hemicoronene–corannulene structure, there are a few other examples in this regard. This includes corannulene hybrids with naphthalene,^{8,9} anthracene,⁹ triphenylene,⁹ benzopyrene,¹⁰ and porphyrin.^{11,12} In most of these cases, distinct property changes are observed in the corannulene nucleus upon its hybridization with the planar unit.¹³

We envisage that by combining the two aforementioned motifs, hybridizing with a polycyclic planar π unit and fluorinating of the aromatic scaffold into a single molecular structure would provide a powerful route to new electronically active corannulene materials. Our recently developed photo-

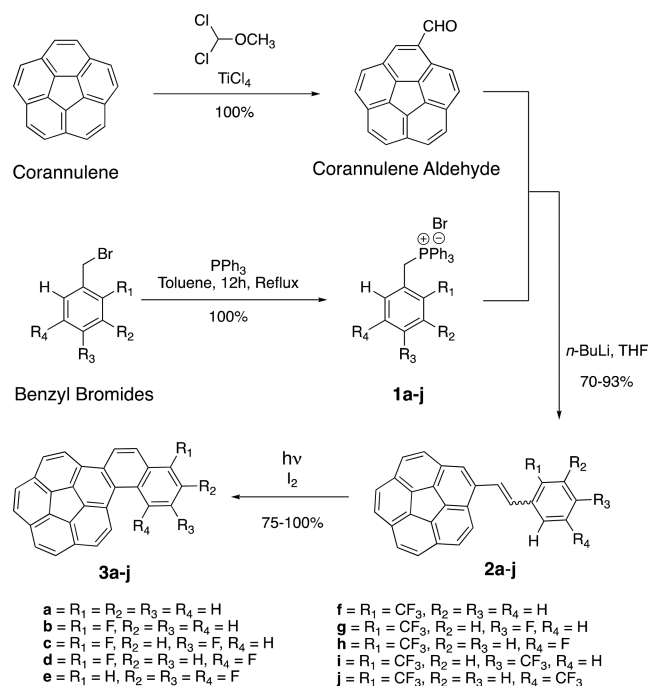
Received: December 14, 2017

chemical synthesis would allow for a facile access to such extended and fluorinated structures due to its high efficiency and modularity.⁸ In this approach, a planar aromatic system of choice can be annulated to the nonplanar corannulene scaffold in a two-step process. First, a vinylene linkage is established between the two segments to be joined together. Next, a photochemically induced oxidative-cyclization process fuses the two aromatic structures together. In the present quest, the planar structure can carry the fluorinated sites, provide the targeted structures with synthetic ease, and would allow for investigations into their electronic properties. This work, therefore, examines the photochemical synthesis of the first family of the extended corannulenes carrying a predefined number, nature, and position of fluorinated sites and their electrochemical and optical properties. Furthermore, a theoretical investigation based on the DFT-calculations is also part of this study and is in agreement with the experimental results.

RESULTS AND DISCUSSION

Synthesis. To accomplish the synthesis, initially, an aldehyde functionality was installed onto corannulene through the Rieche formylation reaction (Scheme 1).¹⁴ This reaction

Scheme 1. Synthesis of Extended and Fluorinated Corannulenes



proceeds to quantitative conversions and does not require a chromatographic purification of the formed product. Hence, multigrams (>10 g) of corannulenealdehyde can be prepared with synthetic ease.

Next, commercially available and inexpensive benzyl bromides having a certain fluorination pattern were converted into phosphonium ylides **1a–j** through treatment with triphenylphosphine. These transformations were also quantitative. Moreover, the formed ylide compounds precipitated out of the reaction and could be simply collected through a simple vacuum filtration process.

Having efficient access to aldehyde and ylide-based building blocks, the Wittig olefination^{15,16} reaction was then carried out to combine corannulene with the fluorinated flat aromatic segment through a vinylene linkage. This process gave rise to the stilbene-like precursors, **2a–j**. Here, the isolated yields ranged from 70 to 93% and column chromatography was necessary to purify the products.

The vinylene precursors, **2a–j**, set the stage for a final oxidative-photocyclization process that would eventually give access to the targeted compounds, **3a–j**.^{17,18} For this transformation, a medium pressure Hg lamp was used as the light source, iodine as an oxidant, and propylene oxide as a quencher for the reaction-produced hydrogen iodide. In general, the photochemical annulation process required a few hours for completion. Once again purification of the final product could be achieved by a simple washing with hexanes. The overall isolated yields for the 10 prepared compounds could be calculated to be in the range of 62–92% over the three synthetic steps. Since these numbers represent unoptimized processes, it is noteworthy that overall isolated yields can reach over 90%. Such efficiency of the synthesis coupled with its practicality is often not associated with the preparation of the complex polycyclic aromatic hydrocarbon derivatives.

Due to several non-chromatographic purifications and high reaction yields, the practicality of the whole synthetic process is such that if multigram quantities of the final products are required, they can be accessed with ease. To demonstrate this aspect, compound **3a** was synthesized in a 1.3-g scale (Figure S1). Such scalability is critical if real life applications, such as in organic electronic devices, are to be targeted using chemistry based on the corannulene motif.

In the prepared series (Chart 1), compound **3a** serves as a control in the follow up electrochemical study. Compounds **3b–e** are derivatives in which one, two, or three fluorine atoms are part of the extended segment. Compounds **3c** and **3d** can be considered as isomers due to 1,3 (*meta*) and 1,4 (*para*)-arrangement of the fluorine atoms. Compound **3f** carries one trifluoromethyl group, and **3g** and **3h** carry an additional fluorine atom at the *meta*- and *para*-position related to the CF₃ group. Lastly, **3i** and **3j** are the compounds carrying two trifluoromethyl groups oriented in the *meta*- and *para*-positions to each other. This diversity of the structures is truly the result of a modular nature of the employed synthetic scheme, in which any ylide compound can be combined to the corannulene scaffold through a Wittig reaction.

Optical Properties. Optical spectroscopy studies revealed that the extension of the corannulene scaffold with the naphthalene unit resulted in a bathochromic shift of 12 nm in the absorption spectrum of **3a** (Figure 1). The introduction of the fluorine atoms resulted into a further shift to the higher wavelengths by 1–7 nm (**3b–i**) (Figure S2). The most red-shifted signal was observed for **3j** at 309 nm. This shift amounted to be about 22 nm when compared to parental corannulene. This is interesting because the placement of the trifluoromethyl groups directly onto the corannulene scaffold is known not to change the optical signature of the core. The fluorescence emission study showed that a weak signal ranging from 400 to 500 nm could be observed for all of the compounds irrespective of the wavelength of excitation (Figure S3).

Electrochemical Properties. Cyclic (CV) and square-wave voltammetry (SWV) were used to examine the electrochemical behavior of **3a–j** and to gauge their electron affinities.

Chart 1. Molecular Structures of the Final Compounds 3a–j

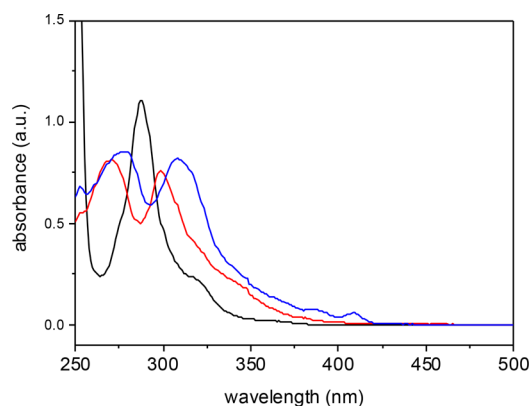
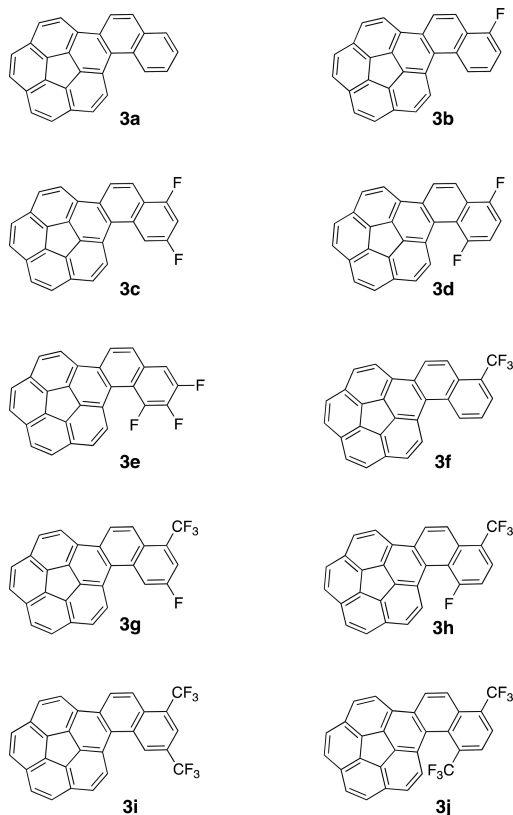


Figure 1. UV–vis spectra of corannulene ($\lambda_{\max} = 287$ nm, black line), **3a** ($\lambda_{\max} = 270$ and 299 nm, red line), and **3j** ($\lambda_{\max} = 278$ and 309 nm, blue line) in tetrahydrofuran at room temperature.

The CV experiments indicated that all of the molecules followed an EEC ($E =$ electron transfer and $C =$ chemical reaction) mechanism (Figure S4). The first electron transfer step produced the anion radicals, which could be further reduced to the dianions at more negative potentials. The dianions were considerably less long-lived than the anion radicals as indicated by how the anodic to cathodic peak current ratio was $\ll 1$. Controlled potential electrolysis experiments also indicated that the first reduction process resulted in the transfer of one electron to produce the anion radical that was stable under the time scale of the experiment ($t = 1800$ s), and they could be oxidized back to the neutral species when a sufficiently positive potential was applied. The reduced species formed at the end of the electrolysis experiment revealed stability over at

least 10 further redox cycles (Figure S5). As can be seen in Figures 2 and S4 and Table 1, pristine corannulene shows a

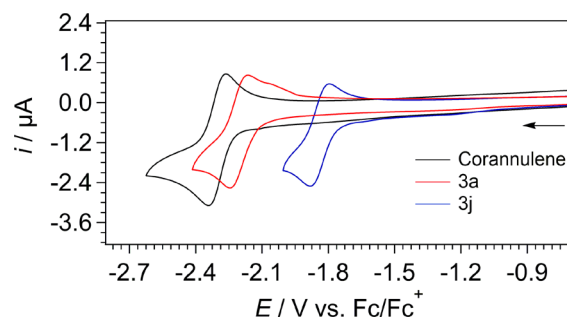


Figure 2. Overlay of cyclic voltammograms showing the first reduction process of 1 mM corannulene (black), **3a** (red), and **3j** (blue) in DMF containing 0.1 M $n\text{Bu}_4\text{NPF}_6$ at a scan rate of 0.1 V s^{-1} using a 1 mm diameter GC working electrode at 298 ± 2 K in a Faraday cage.

Table 1. Measured Reduction Potentials of Corannulene and **3a–j** As Collected Using Square-Wave Voltammetry^a

compound	E^1/V	E^2/V	LUMO/eV
3j	−1.838	−2.195	−2.782
3i	−1.934	−2.115	−2.722
3h	−2.039	−2.452	−2.509
3g	−2.044	−2.488	−2.545
3f	−2.110	−2.311	−2.411
3e	−2.110	−2.457	−2.416
3c	−2.110	−2.331	−2.374
3d	−2.120	−2.336	−2.325
3b	−2.150	−2.674	−2.260
3a	−2.195	−2.744	−2.155
corannulene	−2.306	−2.860	−2.020

^aFirst reduction potentials (bold) are arranged in order of increasing $E_{\text{c}/\text{c}^{\text{red}}}$. Voltammetric measurements were conducted in a Faraday cage with a 1 mm diameter planar GC working electrode in DMF containing 1 mM of compound and 0.1 M $n\text{Bu}_4\text{NPF}_6$ at 298 ± 2 K and recorded with a scan rate of 0.1 V s^{-1} . All values are referenced to the Fc/Fc^+ redox couple. The DFT-computed LUMO energies are listed in the last column for comparison.

chemically reversible first reduction process (${}^1E_{\text{PC}}$) at -2.31 V. The extension of corannulene with naphthalene results in an increase in the first reduction potential by 0.11 V and indicates that **3a** is a better electron acceptor than corannulene. Placement of fluorine atoms on the extended scaffold further enhances the reduction potential (Figure 3). Interestingly, introduction of one CF_3 group, as in the case of **3e**, was found to be as effective as three Ar–F bonds in enhancing the first reduction potential. Addition of Ar–F to one CF_3 group resulted in a further increase in the reduction potential to -2.04 V for compounds **3g–h** (Figure 4). Finally, two CF_3 groups on the extended scaffold **3i–j** show the highest ${}^1E_{\text{PC}}$ in the present series of compounds of -1.93 and -1.84 V. This means that the reduction potential enhancement was approximately 0.46 V when **3j** is compared to pristine corannulene (Figure 2). Although most of the compounds display several reduction processes, only the first two are likely to be associated with the reduction of the starting materials, since the second reduction process was only partially chemically reversible at best (**3a–e**) and, in some cases, appeared to involve multiple electron transfers (**3f–j**).

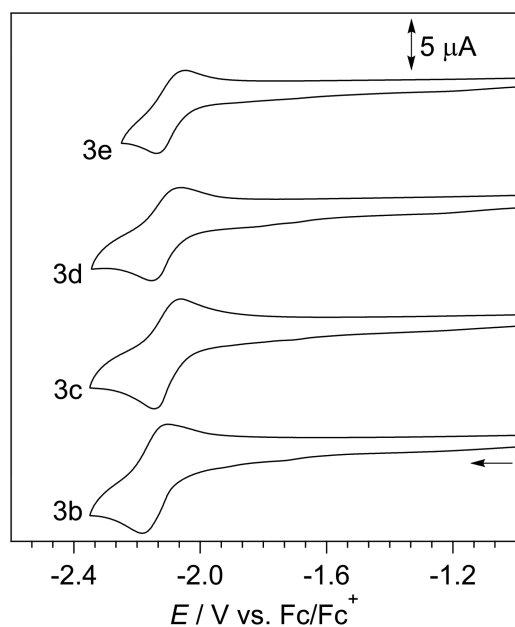


Figure 3. Cyclic voltammograms showing the first reduction process of 1 mM **3b–e** in DMF containing 0.1 M $n\text{Bu}_4\text{NPF}_6$ at a scan rate of 0.1 V s^{-1} using a 1 mm diameter GC working electrode at $298 \pm 2 \text{ K}$ in a Faraday cage.

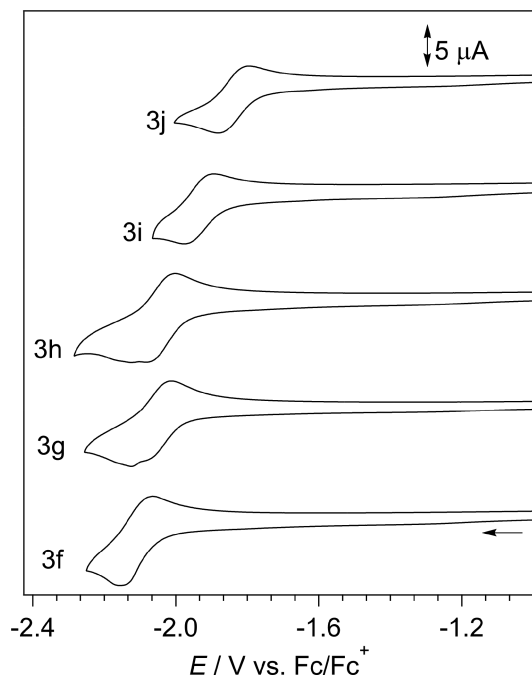


Figure 4. Cyclic voltammograms showing the first reduction process of 1 mM **3f–j** in DMF containing 0.1 M $n\text{Bu}_4\text{NPF}_6$ at a scan rate of 0.1 V s^{-1} using a 1 mm diameter GC working electrode at $298 \pm 2 \text{ K}$ in a Faraday cage.

Computational Studies. The density functional theory (DFT) results are summarized in Figure 5a with the help of a plot between the lowest unoccupied molecular orbital (LUMO) energies and the experimentally measured values of first reduction potentials. The values of LUMO energies are as listed in Table 1. As can be seen from these data, the descending order of LUMO energies is in good agreement with the ascending order of the first reduction potentials. This is

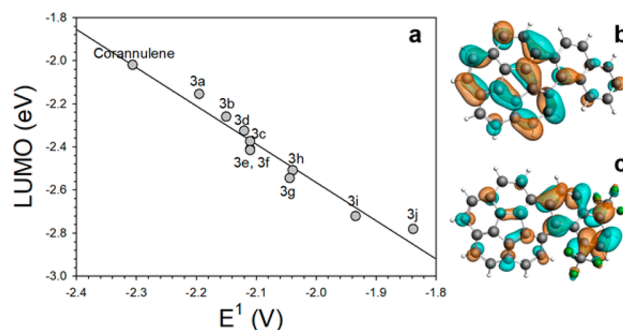


Figure 5. (a) DFT-computed LUMO energy plotted against the first reduction potential measured by CV for corannulene and its derivatives (**3a–j**). Visual representation of the computed LUMO on the molecular skeleton for (b) **3a** and (c) **3j**.

because the negative values of LUMO energies are linearly proportional to the first reduction potentials of the corannulene derivatives. It is also found that LUMO is located more on the fluorinated (and, therefore, the extended) segment of the molecule rather than the corannulene bowl. For example, when **3j** is compared to **3a**, the LUMO is located mostly on the corannulene nucleus (Figure 5b,c). This suggests that the increase in the electron affinity in the present series of the corannulene derivatives can be attributed to the fluorination of the extended aromatic scaffold.

CONCLUSIONS

To summarize, a new family of extended and fluorinated derivatives of corannulene have been prepared through an efficient and modular synthetic scheme. This strategy allows for a large degree of freedom over the choice of the number, nature, and placement of the fluorine atoms on the extended aromatic framework. Furthermore, only one synthetic step in the whole synthesis required a chromatographic purification. Such practicality can be translated to scalability of the synthesis. This aspect is demonstrated through the preparation of one of the family members, **3a**, at a 1.3-g scale. The overall (unoptimized) yields for the preparation of the 10 family members (over three synthetic steps) ranged from 62 to 92%. Optical and electrochemical studies suggest that the electronic properties of the present material family could be systematically tuned and enhanced through adjusting the molecular structure. For instance, a bathochromic shift of 12 nm could be achieved by attaching a naphthalene unit to the corannulene scaffold (**3a**). Placement of two trifluoromethyl groups on this extended part of the molecule allows for a further 10 nm red shift (**3j**). These structural transformations also make the molecules better electron acceptors. For example, **3a** and **3j** show an increase of reduction potential by 0.11 and 0.46 V, respectively, in comparison to pristine corannulene. In essence, the described molecular design concepts can now be applied to efficiently access a new family of electron acceptor materials with adjustable electronic properties and anticipated applications in the arena of organic electronics.

EXPERIMENTAL DETAILS

General Methods. All commercial reagents were used without further purification. Solvents were purified by standard procedures. All reactions with air- and moisture-sensitive reagents were performed in vacuum-dried reaction vessels under nitrogen atmosphere. Column chromatography was carried out on silica gel 40–63 mesh as the stationary phase. Reactions were monitored by thin-layer chromatog-

raphy (TLC) on silica gel-coated aluminum plates (60 F254, Merck) and visualized with UV light ($\lambda = 254$ and 366 nm). ^1H and ^{13}C NMR spectra were recorded with Bruker BBFO-400 and Bruker AV-400 instruments at room temperature by using CDCl_3 as solvent. For ^{13}C NMR measurements in which higher sample concentrations were needed, CS_2 (residual solvent signal = 193 ppm) was added to enhance the solubility of the compounds. Chemical shifts are recorded in parts per million (ppm) relative to tetramethylsilane ($\delta = 0.00$ ppm) and chloroform ($\delta = 7.26$ ppm). ^1H NMR splitting patterns are designated as s (singlet), d (doublet), t (triplet), q (quartet), dd (doublet of doublets), m (multiplet), etc. ^{13}C NMR chemical shifts are reported relative to CDCl_3 ($\delta = 77.00$ ppm). High-resolution mass spectra (HRMS) were recorded by using JEOL Spiral TOF (JMS-S3000) (MALDI) for all starting materials and final compounds. Photocyclization reactions were carried out in 0.5 and 1 L water-cooled immersion-well photochemical reactors equipped with a medium-pressure mercury lamp (125 W).

Voltammetric Measurements. Voltammetric measurements were performed using a Metrohm Autolab PGSTAT302N potentiostat in a three-electrode setup. A 1 mm diameter planar disk glassy carbon disk (GC, Cypress Systems) was used as a working electrode in conjunction with a platinum wire counter electrode (Metrohm) and a silver wire miniature reference electrode (eDAQ) connected to the test solution via a salt bridge containing 0.5 M tetra-*n*-butylammonium hexafluorophosphate ($n\text{Bu}_4\text{NPF}_6$) in DMF (Tedia). $n\text{Bu}_4\text{NPF}_6$ was synthesized through a standard procedure according to the literature¹⁹ and used as the supporting electrolyte. All voltammetric experiments were conducted under an argon atmosphere at room temperature in a Faraday cage. Prior to each scan, the working electrode was cleaned by polishing it with an alumina oxide (grain size $0.3 \mu\text{m}$) slurry on a Buehler Ultrapad polishing cloth, rinsing it with acetone, and then drying it with a lint free tissue. In accordance with IUPAC recommendations, the absolute potentials were calibrated using ferrocene (Fc) as an internal reference which was added to the test solution at the end of the measurements.

Controlled-Potential Electrolysis. Controlled potential electrolysis experiments were conducted in a two-compartment electrolysis cell separated by a sintered glass frit with a porosity number 5 (1.0 – $1.7 \mu\text{m}$). Two symmetrically arranged and identically sized hollow, cylindrical GC rods (working and auxiliary electrodes) were used. The silver wire miniature reference electrode (eDAQ) was connected to the test solution via a salt bridge containing 0.5 M $n\text{Bu}_4\text{NPF}_6$ in DMF. The volume of the solutions in both the counter and working electrode compartments were 25 mL, and stirring was induced via forced convection through bubbling with argon and N_2 at room temperature (298 ± 2 K). The total number of electrons transferred during CPE was calculated from the following equation: $n = Q/NF$, where N = the number of moles of the starting material used, Q = the charge (in coulombs), n = the number of electrons, and F is the Faraday constant (96485 C/mol).

General Procedure for the Synthesis of Triphenylphosphonium Salts 1a–j. Triphenylphosphine (1.2 equiv) was added to a stirred solution of a commercially available derivatives of benzyl bromide (300 mg, 1.0 equiv) in 20 mL toluene, and the reaction mixture was refluxed for 12 h. After completion of reaction, the reaction mixture was cooled to room temperature and the resulting phosphonium salt precipitate was collected by filtration and dried. In all cases, the isolated chemical yields were quantitative.

General Procedure for the Synthesis of Stilbene-like Vinylene Derivatives 2a–j through the Wittig Reaction. As a typical procedure, $n\text{-BuLi}$ (2.0 M solution in hexane) was added to a vacuum-dried round-bottom flask containing a suspension of benzyltriphenylphosphonium bromide (0.66 mmol) in 35 mL of dry THF (0.330 mL) at 0°C under a N_2 atmosphere. The mixture was stirred for 30 min. Corannulene-carbaldehyde (0.44 mmol) in 5 mL of dry THF was added, and the solution was stirred at room temperature for 2–3 h. The progress of the reaction was monitored by TLC. After completion of the reaction, the reaction mixture was quenched with water and then extracted with CH_2Cl_2 (3×100 mL). The combined organic layers were dried (anhydrous Na_2SO_4) and concentrated. The

residue was purified by column chromatography using mixture of hexane/EtOAc to give the corannulene vinylenes as a mixture of *trans/cis* isomers. The isolated chemical yields ranged from 70 to 93%.

2a. Yield: 92% (1.4 g). Yellow solid. mp 206 – 208°C . ^1H NMR (400 MHz, CDCl_3 , δ): 8.17 (d, $J = 8.8$ Hz, 1H), 7.94 (s, 1H), 7.90–7.73 (m, 8H), 7.68 (d, $J = 7.5$ Hz, 2H), 7.53 (d, $J = 16.2$ Hz, 1H), 7.45 (t, $J = 7.6$ Hz, 2H), 7.34 (t, $J = 7.3$ Hz, 1H). ^{13}C NMR (101 MHz, CDCl_3 , δ): 137.7, 137.6, 136.4, 136.1, 135.8, 135.6, 135.5, 133.1, 131.09, 131.05, 130.9, 129.2, 128.9, 128.1, 127.6, 127.5, 127.4, 127.2, 127.1, 127.09, 127.01, 126.9, 126.7, 125.8, 124.5. HRMS (MALDI-TOF) (m/z): $[M]^+$ calcd for $\text{C}_{28}\text{H}_{16}$, 352.1247; found, 352.1247.

2b. Yield: 73% (120 mg). Light yellow solid. mp 104 – 106°C . *trans:cis* ratio 1:1. ^1H NMR (400 MHz, CDCl_3 , δ): 8.17 (d, $J = 8.8$ Hz, 1H), 7.97 (s, 1H), 7.91–7.62 (m, 18H), 7.42 (t, $J = 7.7$ Hz, 1H), 7.30 (dd, $J = 12.1$, 5.7 Hz, 2H), 7.24–6.98 (m, 6H), 6.82 (t, $J = 7.5$ Hz, 1H). ^{13}C NMR (101 MHz, CDCl_3 , δ): 161.9, 159.4, 137.4, 136.3, 136.2, 135.9, 135.7, 135.6 (d, $J = 3.5$ Hz), 135.5, 135.45, 135.43, 132.2, 132.1, 131.1 (d, $J = 3.3$ Hz), 130.9, 130.87, 130.83 (d, $J = 2.5$ Hz), 130.7 (d, $J = 2.4$ Hz), 130.6, 129.5, 129.4, 129.2 (d, $J = 8.5$ Hz), 129.0, 128.8 (d, $J = 5.1$ Hz), 127.6, 127.4, 127.3 (d, $J = 3.0$ Hz), 127.2 (d, $J = 1.7$ Hz), 127.1, 127.0, 126.96, 126.91, 125.9, 125.6, 125.4, 125.3, 125.1 (d, $J = 3.5$ Hz), 125.0 (d, $J = 4.0$ Hz), 124.8, 124.3 (d, $J = 3.5$ Hz), 123.7 (d, $J = 3.6$ Hz), 116.1, 115.9, 115.7, 115.5. ^{19}F NMR (282 MHz, CDCl_3 , δ): -115.38 to -115.52 (m, $J = 8.2$, 5.9 Hz), -117.34 (ddd, $J = 10.8$, 7.7, 5.2 Hz). HRMS (MALDI-TOF) (m/z): $[M]^+$ calcd for $\text{C}_{28}\text{H}_{15}\text{F}$, 370.1158; found, 370.1162.

2c. Yield: 78% (129 mg). Orange foamy solid. mp 78 – 80°C . *trans:cis* ratio 6:5. ^1H NMR (400 MHz, CDCl_3 , δ): 8.14 (d, $J = 8.8$ Hz, 3H), 7.94 (s, 3H), 7.90–7.66 (m, 40H), 7.58 (dd, $J = 15.9$, 7.1 Hz, 4H), 7.39 (dd, $J = 15.4$, 8.7 Hz, 1H), 7.20–7.05 (m, 2H), 7.01–6.76 (m, 10H), 6.73–6.65 (m, 1H), 6.57 (t, $J = 7.3$ Hz, 1H). ^{13}C NMR (101 MHz, CDCl_3 , δ): 163.7, 163.6, 161.9, 161.8, 161.2, 161.1, 159.4, 159.3, 137.3, 136.3, 135.9, 135.7, 135.5, 131.0, 130.83, 130.80, 130.7, 129.4, 128.5 (dd, $J = 5.1$, 2.4 Hz), 128.1 (dd, $J = 9.5$, 5.2 Hz), 127.6, 127.4, 127.3, 127.15, 127.07, 127.03 (dd, $J = 12.2$, 3.9 Hz), 127.0, 126.9, 126.8, 126.7, 126.6, 126.5, 126.4, 126.3, 126.2, 126.1, 126.0, 125.9, 125.8, 125.7, 125.6, 125.5, 125.4, 125.3, 125.2, 125.1, 125.0, 124.9, 124.8, 124.7, 124.6, 124.5, 124.4, 124.3, 124.2, 124.1, 124.0, 123.9, 123.8, 123.7, 123.6, 123.5, 123.4, 123.3, 123.2, 123.1, 123.0, 122.9, 122.8, 122.7, 122.6, 122.5, 122.4, 122.3, 122.2, 122.1, 122.0, 121.9, 121.8, 121.7, 121.6, 121.5, 121.4, 121.3, 121.2, 121.1, 121.0, 120.9, 120.8, 120.7, 120.6, 120.5, 120.4, 120.3, 120.2, 120.1, 120.0, 119.9, 119.8, 119.7, 119.6, 119.5, 119.4, 119.3, 119.2, 119.1, 119.0, 118.9, 118.8, 118.7, 118.6, 118.5, 118.4, 118.3, 118.2, 118.1, 118.0, 117.9, 117.8, 117.7, 117.6, 117.5, 117.4, 117.3, 117.2, 117.1, 117.0, 116.9, 116.8, 116.7, 116.6, 116.5, 116.4, 116.3, 116.2, 116.1, 116.0, 115.9, 115.8, 115.7, 115.6, 115.5, 115.4, 115.3, 115.2, 115.1, 115.0, 114.9, 114.8, 114.7, 114.6, 114.5, 114.4, 114.3, 114.2, 114.1, 114.0, 113.9, 113.8, 113.7, 113.6, 113.5, 113.4, 113.3, 113.2, 113.1, 113.0, 112.9, 112.8, 112.7, 112.6, 112.5, 112.4, 112.3, 112.2, 112.1, 112.0, 111.9, 111.8, 111.7, 111.6, 111.5, 111.4, 111.3, 111.2, 111.1, 111.0, 110.9, 110.8, 110.7, 110.6, 110.5, 110.4, 110.3, 110.2, 110.1, 110.0, 109.9, 109.8, 109.7, 109.6, 109.5, 109.4, 109.3, 109.2, 109.1, 109.0, 108.9, 108.8, 108.7, 108.6, 108.5, 108.4, 108.3, 108.2, 108.1, 108.0, 107.9, 107.8, 107.7, 107.6, 107.5, 107.4, 107.3, 107.2, 107.1, 107.0, 106.9, 106.8, 106.7, 106.6, 106.5, 106.4, 106.3, 106.2, 106.1, 106.0, 105.9, 105.8, 105.7, 105.6, 105.5, 105.4, 105.3, 105.2, 105.1, 105.0, 104.9, 104.8, 104.7, 104.6, 104.5, 104.4, 104.3, 104.2, 104.1, 104.0, 103.9, 103.8, 103.7, 103.6, 103.5, 103.4, 103.3, 103.2, 103.1, 103.0, 102.9, 102.8, 102.7, 102.6, 102.5, 102.4, 102.3, 102.2, 102.1, 102.0, 101.9, 101.8, 101.7, 101.6, 101.5, 101.4, 101.3, 101.2, 101.1, 101.0, 100.9, 100.8, 100.7, 100.6, 100.5, 100.4, 100.3, 100.2, 100.1, 100.0, 99.9, 99.8, 99.7, 99.6, 99.5, 99.4, 99.3, 99.2, 99.1, 99.0, 98.9, 98.8, 98.7, 98.6, 98.5, 98.4, 98.3, 98.2, 98.1, 98.0, 97.9, 97.8, 97.7, 97.6, 97.5, 97.4, 97.3, 97.2, 97.1, 97.0, 96.9, 96.8, 96.7, 96.6, 96.5, 96.4, 96.3, 96.2, 96.1, 96.0, 95.9, 95.8, 95.7, 95.6, 95.5, 95.4, 95.3, 95.2, 95.1, 95.0, 94.9, 94.8, 94.7, 94.6, 94.5, 94.4, 94.3, 94.2, 94.1, 94.0, 93.9, 93.8, 93.7, 93.6, 93.5, 93.4, 93.3, 93.2, 93.1, 93.0, 92.9, 92.8, 92.7, 92.6, 92.5, 92.4, 92.3, 92.2, 92.1, 92.0, 91.9, 91.8, 91.7, 91.6, 91.5, 91.4, 91.3, 91.2, 91.1, 91.0, 90.9, 90.8, 90.7, 90.6, 90.5, 90.4, 90.3, 90.2, 90.1, 90.0, 89.9, 89.8, 89.7, 89.6, 89.5, 89.4, 89.3, 89.2, 89.1, 89.0, 88.9, 88.8, 88.7, 88.6, 88.5, 88.4, 88.3, 88.2, 88.1, 88.0, 87.9, 87.8, 87.7, 87.6, 87.5, 87.4, 87.3, 87.2, 87.1, 87.0, 86.9, 86.8, 86.7, 86.6, 86.5, 86.4, 86.3, 86.2, 86.1, 86.0, 85.9, 85.8, 85.7, 85.6, 85.5, 85.4, 85.3, 85.2, 85.1, 85.0, 84.9, 84.8, 84.7, 84.6, 84.5, 84.4, 84.3, 84.2, 84.1, 84.0, 83.9, 83.8, 83.7, 83.6, 83.5, 83.4, 83.3, 83.2, 83.1, 83.0, 82.9, 82.8, 82.7, 82.6, 82.5, 82.4, 82.3, 82.2, 82.1, 82.0, 81.9, 81.8, 81.7, 81.6, 81.5, 81.4, 81.3, 81.2, 81.1, 81.0, 80.9, 80.8, 80.7, 80.6, 80.5, 80.4, 80.3, 80.2, 80.1, 80.0, 79.9, 79.8, 79.7, 79.6, 79.5, 79.4, 79.3, 79.2, 79.1, 79.0, 78.9, 78.8, 78.7, 78.6, 78.5, 78.4, 78.3, 78.2, 78.1, 78.0, 77.9, 77.8, 77.7, 77.6, 77.5, 77.4, 77.3, 77.2, 77.1, 77.0, 76.9, 76.8, 76.7, 76.6, 76.5, 76.4, 76.3, 76.2, 76.1, 76.0, 75.9, 75.8, 75.7, 75.6, 75.5, 75.4, 75.3, 75.2, 75.1, 75.0, 74.9, 74.8, 74.7, 74.6, 74.5, 74.4, 74.3, 74.2, 74.1, 74.0, 73.9, 73.8, 73.7, 73.6, 73.5, 73.4, 73.3, 73.2, 73.1, 73.0, 72.9, 72.8, 72.7, 72.6, 72.5, 72.4, 72.3, 72.2, 72.1, 72.0, 71.9, 71.8, 71.7, 71.6, 71.5, 71.4, 71.3, 71.2, 71.1, 71.0, 70.9, 70.8, 70.7, 70.6, 70.5, 70.4, 70.3, 70.2, 70.1, 70.0, 69.9, 69.8, 69.7, 69.6, 69.5, 69.4, 69.3, 69.2, 69.1, 69.0, 68.9, 68.8, 68.7, 68.6, 68.5, 68.4, 68.3, 68.2, 68.1, 68.0, 67.9, 67.8, 67.7, 67.6, 67.5, 67.4, 67.3, 67.2, 67.1, 67.0, 66.9, 66.8, 66.7, 66.6, 66.5, 66.4, 66.3, 66.2, 66.1, 66.0, 65.9, 65.8, 65.7, 65.6, 65.5, 65.4, 65.3, 65.2, 65.1, 65.0, 64.9, 64.8, 64.7, 64.6, 64.5, 64.4, 64.3, 64.2, 64.1, 64.0, 63.9, 63.8, 63.7, 63.6, 63.5, 63.4, 63.3, 63.2, 63.1, 63.0, 62.9, 62.8, 62.7, 62.6, 62.5, 62.4, 62.3, 62.2, 62.1, 62.0, 61.9, 61.8, 61.7, 61.6, 61.5, 61.4, 61.3, 61.2, 61.1, 61.0, 60.9, 60.8, 60.7, 60.6, 60.5, 60.4, 60.3, 60.2, 60.1, 60.0, 59.9, 59.8, 59.7, 59.6, 59.5, 59.4, 59.3, 59.2, 59.1, 59.0, 58.9, 58.8, 58.7, 58.6, 58.5, 58.4, 58.3, 58.2, 58.1, 58.0, 57.9, 57.8, 57.7, 57.6, 57.5, 57.4, 57.3, 57.2, 57.1, 57.0, 56.9, 56.8, 56.7, 56.6, 56.5, 56.4, 56.3, 56.2, 56.1, 56.0, 55.9, 55.8, 55.7, 55.6, 55.5, 55.4, 55.3, 55.2, 55.1, 55.0, 54.9, 54.8, 54.7, 54.6, 54.5, 54.4, 54.3, 54.2, 54.1, 54.0, 53.9, 53.8, 53.7, 53.6, 53.5, 53.4, 53.3, 53.2, 53.1, 53.0, 52.9, 52.8, 52.7, 52.6, 52.5, 52.4, 52.3, 52.2, 52.1, 52.0, 51.9, 51.8, 51.7, 51.6, 51.5, 51.4, 51.3, 51.2, 51.1, 51.0, 50.9, 50.8, 50.7, 50.6, 50.5, 50.4, 50.3, 50.2, 50.1, 50.0, 49.9, 49.8, 49.7, 49.6, 49.5, 49.4, 49.3, 49.2, 49.1, 49.0, 48.9, 48.8, 48.7, 48.6, 48.5, 48.4, 48.3, 48.2, 48.1, 48.0, 47.9, 47.8, 47.7, 47.6, 47.5, 47.4, 47.3, 47.2, 47.1, 47.0, 46.9, 46.8, 46.7, 46.6, 46.5, 46.4, 46.3, 46.2, 46.1, 46.0, 45.9, 45.8, 45.7, 45.6, 45.5, 45.4, 45.3, 45.2, 45.1, 45.0, 44.9, 44.8, 44.7, 44.6, 44.5, 44.4, 44.3, 44.2, 44.1, 44.0, 43.9, 43.8, 43.7, 43.6, 43.5, 43.4, 43.3, 43.2, 43.1, 43.0, 42.9, 42.8, 42.7, 42.6, 42.5, 42.4, 42.3, 42.2, 42.1, 42.0, 41.9, 41.8, 41.7, 41.6, 41.5, 41.4, 41.3, 41.2, 41.1, 41.0, 40.9, 40.8, 40.7, 40.6, 40.5, 40.4, 40.3, 40.2, 40.1, 40.0, 39.9, 39.8, 39.7, 39.6, 39.5, 39.4, 39.3, 39.2, 39.1, 39.0, 38.9, 38.8, 38.7, 38.6, 38.5, 38.4, 38.3, 38.2, 38.1, 38.0, 37.9, 37.8, 37.7, 37.6, 37.5, 37.4, 37.3, 37.2, 37.1, 37.0, 36.9, 36.8, 36.7, 36.6, 36.5, 36.4, 36.3, 36.2, 36.1, 36.0, 35.9, 35.8, 35.7, 35.6, 35.5, 35.4, 35.3, 35.2, 35.1, 35.0, 34.9, 34.8, 34.7, 34.6, 34.5, 34.4, 34.3, 34.2, 34.1, 34.0, 33.9, 33.8, 33.7, 33.6, 33.5, 33.4, 33.3, 33.2, 33.1, 33.0, 32.9, 32.8, 32.7, 32.6, 32.5, 32.4, 32.3, 32.2, 32.1, 32.0, 31.9, 31.8, 31.7, 31.6, 31.5, 31.4, 31.3, 31.2, 31.1, 31.0, 30.9, 30.8, 30.7, 30.6, 30.5, 30.4, 30.3, 30.2, 30.1, 30.0, 29.9, 29.8, 29.7, 29.6, 29.5, 29.4, 29.3, 29.2, 29.1, 29.0, 28.9, 28.8, 28.7, 28.6, 28.5, 28.4, 28.3, 28.2, 28.1, 28.0, 27.9, 27.8, 27.7, 27.6, 27.5, 27.4, 27.3, 27.2, 27.1, 27.0, 26.9, 26.8, 26.7, 26.6, 26.5, 26.4, 26.3, 26.2, 26.1, 26.0, 25.9, 25.8, 25.7, 25.6, 25.5, 25.4, 25.3, 25.2, 25.1, 25.0, 24.9, 24.8, 24.7, 24.6, 24.5, 24.4, 24.3, 24.2, 24.1, 24.0, 23.9, 23.8, 23.7, 23.6, 23.5, 23.4, 23.3, 23.2, 23.1, 23.0, 22.9, 22.8, 22.7, 22.6, 22.5, 22.4, 22.3, 22.2, 22.1, 22.0, 21.9, 21.8, 21.7, 21.6, 21.5, 21.4, 21.3, 21.2, 21.1, 21.0, 20.9, 20.8, 20.7, 20.6, 20.5, 20.4, 20.3, 20.2, 20.1, 20.0, 19.9, 19.8, 19.7, 19.6, 19.5, 19.4, 19.3, 19.2, 19.1, 19.0, 18.9, 18.8, 18.7, 18.6, 18.5, 18.4, 18.3, 18.2, 18.1, 18.0, 17.9, 17.8, 17.7, 17.6, 17.5, 17.4, 17.3, 17.2, 17.1, 17.0, 16.9, 16.8, 16.7, 16.6, 16.5, 16.4, 16.3, 16.2, 16.1, 16.0, 15.9, 15.8, 15.7, 15.6, 15.5, 15.4, 15.3, 15.2, 15.1, 15.0, 14.9, 14.8, 14.7, 14.6, 14.5, 14.4, 14.3, 14.2, 14.1, 14.0, 13.9, 13.8, 13.7, 13.6, 13.5, 13.4, 13.3, 13.2, 13.1, 13.0, 12.9, 12.8, 12.7, 12.6, 12.5, 12.4, 12.3, 12.2, 12.1, 12.0, 11.9, 11.8, 11.7, 11.6, 11.5, 11.4, 11.3, 11.2, 11.1, 11.0, 10.9, 10.8, 10.7, 10.6, 10.5, 10.4, 10.3, 10.2, 10.1, 10.0, 9.9, 9.8, 9.7, 9.6, 9.5, 9.4, 9.3, 9.2, 9.1, 9.0, 8.9, 8.8, 8.7, 8.6, 8.5, 8.4, 8.3, 8.2, 8.1, 8.0, 7.9, 7.8, 7.7, 7.6, 7.5, 7.4, 7.3, 7.2, 7.1, 7.0, 6.9, 6.8, 6.7, 6.6, 6.5, 6.4, 6.3, 6.2, 6.1, 6.0, 5.9, 5.8, 5.7, 5.6, 5.5, 5.4, 5.3, 5.2, 5.1, 5.0, 4.9, 4.8, 4.7, 4.6, 4.5, 4.4, 4.3, 4.2, 4.1, 4.0, 3.9, 3.8, 3.7, 3.6, 3.5, 3.4, 3.3, 3.2, 3.1, 3.0, 2.9, 2.8, 2.7, 2.6, 2.5, 2.4, 2.3, 2.2, 2.1, 2.0, 1.9, 1.8, 1.7, 1.6, 1.5, 1.4, 1.3, 1.2, 1.1, 1.0, 0.9, 0.8, 0.7, 0.6, 0.5, 0.4, 0.3, 0.2, 0.1, 0.0.

2d. Yield: 77% (128 mg). Orange foamy solid. mp 80 – 82°C . *trans:cis* ratio 6:5. ^1H NMR (400 MHz, CDCl_3 , δ): 8.15 (d, $J = 8.8$ Hz, 4H), 7.96 (d, $J = 6.4$ Hz, 4H), 7.91–7.73 (m, 47H), 7.69 (dd, $J = 5.9$, 2.7 Hz, 6H), 7.62 (d, $J = 16.4$ Hz, 4H), 7.44 (ddd, $J = 9.0$, 5.7, 3.0 Hz, 4H), 7.21–6.90 (m, 18H), 6.89–6.80 (m, 3H), 6.72 (s, 1H). ^{13}C NMR (101 MHz, CDCl_3 , δ): 160.8 (d, $J = 2.3$ Hz), 157.8 (d, $J = 2.4$ Hz), 155.3 (d, $J = 2.3$ Hz), 136.8, 136.3, 135.9, 135.7, 135.6, 135.4, 130.97, 130.90, 130.7, 130.6, 129.9 (d, $J = 4.6$ Hz), 128.8, 127.7, 127.5, 127.4, 127.0, 126.9, 125.6, 125.4, 125.2, 124.

(ddd, $J = 31.7, 20.4, 8.4$ Hz), -133.74 to -134.00 (m), -134.15 to -134.36 (m), -159.44 to -159.70 (m), -159.96 to -160.20 (m), -160.38 to -160.71 (m), -160.85 (tt, $J = 20.7, 6.5$ Hz). HRMS (MALDI-TOF) (m/z): $[M]^+$ calcd for $C_{28}H_{13}F_3$, 406.0963; found, 406.0944.

2f. Yield: 93% (160 mg). Yellow solid. mp 140–141 °C. *trans:cis* ratio 1:1. 1H NMR (400 MHz, $CDCl_3$, δ): 8.16 (d, $J = 8.8$ Hz, 1H), 7.96 (d, $J = 5.4$ Hz, 2H), 7.92 (d, $J = 2.2$ Hz, 1H), 7.87 (dd, $J = 9.2, 6.4$ Hz, 2H), 7.79 (ddd, $J = 17.0, 8.3, 6.2$ Hz, 14H), 7.71–7.58 (m, 4H), 7.57 (s, 1H), 7.44 (dd, $J = 15.2, 7.6$ Hz, 2H), 7.23 (t, $J = 6.2$ Hz, 2H), 7.16 (t, $J = 7.6$ Hz, 1H). ^{13}C NMR (101 MHz, $CDCl_3$, δ): 137.0, 136.5 (d, $J = 1.5$ Hz), 136.3, 136.2, 136.1 (d, $J = 1.8$ Hz), 136.0, 135.8, 135.7, 135.65, 135.62, 135.57, 135.51, 135.47, 135.41, 132.1, 132.0 (d, $J = 0.6$ Hz), 131.4 (d, $J = 0.4$ Hz), 130.99, 130.92, 130.89, 130.87, 130.78, 130.71, 130.67, 130.65, 130.63, 129.9, 129.5, 129.1 (d, $J = 0.9$ Hz), 128.9, 128.7, 128.4 (d, $J = 2.0$ Hz), 127.9, 127.75, 127.73, 127.6, 127.5, 127.4, 127.3, 127.1 (ddd, $J = 16.8, 11.8, 2.6$ Hz), 126.1 (dd, $J = 11.9, 6.1$ Hz), 125.97, 125.95, 125.93, 125.6, 125.5 (d, $J = 1.3$ Hz), 123.2 (d, $J = 4.1$ Hz). ^{19}F NMR (282 MHz, $CDCl_3$, δ): -59.30 (s), -60.49 (s). HRMS (MALDI-TOF) (m/z): $[M]^+$ calcd for $C_{29}H_{15}F_3$, 420.1126; found, 420.1121.

2g. Yield: 89% (150 mg). Yellow solid. mp 134–136 °C. *trans:cis* ratio 20:3. 1H NMR (400 MHz, $CDCl_3$, δ): 8.14 (d, $J = 8.8$ Hz, 4H), 7.95 (s, 4H), 7.92–7.56 (m, 50H), 7.21–7.14 (m, 1H), 7.14–7.06 (m, 4H), 7.01–6.91 (m, 1H). ^{13}C NMR (101 MHz, $CDCl_3$, δ): 165.9, 165.1, 163.5, 162.6, 139.4 (dd, $J = 8.5, 1.3$ Hz), 139.1 (d, $J = 9.0$ Hz), 136.4, 136.3, 136.2, 135.9, 135.8, 135.76, 135.69, 135.63–135.55 (m), 135.4, 134.9, 131.9, 131.1, 131.0 (d, $J = 1.1$ Hz), 130.93, 130.86, 130.79, 130.65, 130.56, 129.2, 128.74, 128.69–128.37 (m), 127.9, 127.8, 127.5, 127.4, 127.34, 127.25, 127.19, 127.11, 127.04, 126.94, 126.9, 126.0, 125.6, 125.3, 124.1, 123.8, 122.9, 119.2, 118.9, 114.5 (d, $J = 2.6$ Hz), 114.2 (d, $J = 2.5$ Hz), 113.9, 113.7. ^{19}F NMR (282 MHz, $CDCl_3$, δ): -58.62 (s), -59.78 (s). HRMS (MALDI-TOF) (m/z): $[M]^+$ calcd for $C_{29}H_{14}F_4$, 438.1032; found, 438.1033.

2h. Yield: 85% (143 mg). Yellow solid. mp 143–145 °C. *trans:cis* ratio 1:1. 1H NMR (400 MHz, $CDCl_3$, δ): 8.13 (d, $J = 8.8$ Hz, 1H), 7.96–7.90 (m, 2H), 7.88–7.72 (m, 13H), 7.71–7.61 (m, 4H), 7.56 (s, 1H), 7.45 (ddd, $J = 14.4, 8.8, 5.6$ Hz, 3H), 7.33 (td, $J = 8.3, 2.6$ Hz, 1H), 7.23 (d, $J = 12.2$ Hz, 1H), 7.13 (d, $J = 14.1$ Hz, 1H), 6.86 (td, $J = 8.4, 2.7$ Hz, 1H). ^{13}C NMR (101 MHz, $CDCl_3$, δ): 162.8, 162.4, 160.3, 159.9, 136.8, 136.3, 136.2, 135.9, 135.8, 135.73–135.60 (m), 135.5, 135.4, 135.3, 134.2 (d, $J = 7.8$ Hz), 132.7, 132.1, 130.98 (d, $J = 2.0$ Hz), 130.93, 130.86, 130.77, 130.67, 130.65, 130.61, 130.3, 129.3, 129.2 (d, $J = 7.8$ Hz), 128.8, 127.9, 127.8, 127.7, 127.5, 127.39, 127.38, 127.33, 127.25, 127.17, 127.11, 127.0, 126.92, 126.90, 125.5 (d, $J = 4.3$ Hz), 125.4, 119.2, 119.0, 118.6, 118.4, 113.97–113.47 (m). ^{19}F NMR (282 MHz, $CDCl_3$, δ): -59.86 (s), -61.01 (s). HRMS (MALDI-TOF) (m/z): $[M]^+$ calcd for $C_{29}H_{14}F_4$, 438.1032; found, 438.1024.

2i. Yield: 89% (152 mg). Yellow solid. mp 165–167 °C. *trans:cis* ratio 1:1. 1H NMR (400 MHz, $CDCl_3$, δ): 8.14 (d, $J = 8.9$ Hz, 1H), 8.08 (d, $J = 8.3$ Hz, 1H), 7.99 (d, $J = 9.1$ Hz, 3H), 7.93–7.86 (m, 3H), 7.86–7.74 (m, 12H), 7.74–7.62 (m, 3H), 7.58 (d, $J = 8.1$ Hz, 1H), 7.55 (d, $J = 1.0$ Hz, 1H), 7.41 (d, $J = 8.1$ Hz, 1H), 7.35 (dd, $J = 12.1, 0.9$ Hz, 1H), 7.18 (d, $J = 11.5$ Hz, 1H). ^{13}C NMR (101 MHz, $CDCl_3$, δ): 140.1, 140.0, 136.4, 136.2 (d, $J = 2.4$ Hz), 136.0, 135.9, 135.8, 135.7 (d, $J = 3.4$ Hz), 135.6 (d, $J = 3.5$ Hz), 135.4, 134.8, 133.1, 132.8, 131.9, 131.1 (d, $J = 2.3$ Hz), 131.0, 130.9, 130.8 (d, $J = 3.5$ Hz), 130.7, 130.5 (d, $J = 3.0$ Hz), 129.8, 129.4, 129.29, 129.24, 129.1, 128.8 (d, $J = 3.2$ Hz), 128.7, 128.4, 128.1, 127.9, 127.7, 127.6, 127.5, 127.4, 127.3, 127.2, 127.1, 127.0, 126.95, 126.94, 126.8, 126.7, 126.3, 125.2, 125.1, 123.4, 122.4. ^{19}F NMR (282 MHz, $CDCl_3$, δ): -59.88 (s), -61.00 (s), -62.92 (d, $J = 37.3$ Hz). HRMS (MALDI-TOF) (m/z): $[M]^+$ calcd for $C_{30}H_{14}F_6$, 488.1000; found, 488.0999.

2j. Yield: 70% (120 mg). Yellow solid. mp 133–134 °C. *trans:cis* ratio 3:4. 1H NMR (400 MHz, $CDCl_3$, δ): 8.18 (s, 1H), 8.15 (d, $J = 8.9$ Hz, 1H), 7.98 (s, 1H), 7.91 (s, 1H), 7.90–7.76 (m, 18H), 7.74 (dd, $J = 7.0, 5.6$ Hz, 2H), 7.71–7.63 (m, 3H), 7.59 (dd, $J = 4.9, 4.0$ Hz, 2H), 7.52 (d, $J = 8.2$ Hz, 1H), 7.31 (dt, $J = 7.2, 3.6$ Hz, 1H), 7.18 (dd, $J = 12.1, 2.3$ Hz, 1H). ^{13}C NMR (101 MHz, $CDCl_3$, δ): 137.6, 137.3, 136.39, 136.33, 136.2, 136.0, 135.9, 135.2, 135.7 (d, $J = 1.9$ Hz), 135.6

(d, $J = 4.0$ Hz), 135.4, 134.6, 132.6, 131.8, 131.1, 131.0 (d, $J = 1.4$ Hz), 130.9, 130.8, 130.5 (d, $J = 3.1$ Hz), 129.3 (dd, $J = 7.3, 3.6$ Hz), 129.0, 128.7, 127.9 (d, $J = 3.2$ Hz), 127.6, 127.5, 127.4, 127.34, 127.32, 127.28, 127.21, 127.09, 127.03, 126.9, 126.8 (d, $J = 1.7$ Hz), 126.7, 126.3, 125.3, 125.2, 124.3, 124.12–123.81 (m), 122.4. ^{19}F NMR (282 MHz, $CDCl_3$, δ): -60.00 (s), -61.05 (s), -63.28 (s), -63.87 (s). HRMS (MALDI-TOF) (m/z): $[M]^+$ calcd for $C_{30}H_{14}F_6$, 488.0994; found, 488.0974.

General Procedure for Oxidative Photocyclizations. As a typical procedure, a solution containing corannulene vinylene (0.135 mmol), I_2 (37.7 mg, 0.148 mmol), and propylene-oxide (0.95 mL, 100 equiv 100.0 equiv) in 125 mL of toluene was irradiated in a photoreactor fitted with a water-cooled immersion flask and a medium-pressure Hg lamp (125 W) under a N_2 atmosphere. The progress of the reaction was monitored by disappearance of the iodine color as well as by TLC (Hex/EtOAc 7/3). After the reaction completion (3–4 h), the reaction mixture was quenched with saturated $Na_2S_2O_3$ and extracted. The aqueous solution was extracted again with CH_2Cl_2 (4 \times 20 mL). The combined organic layers were dried (anhydrous Na_2SO_4) and concentrated. The products were purified by washing with hexane several times.

3a. Yield: 98% (1.36 g). Beige solid. mp 256–257 °C. 1H NMR (400 MHz, $CDCl_3$, δ): 9.50 (d, $J = 8.5$ Hz, 1H), 8.67 (dd, $J = 8.8, 2.0$ Hz, 2H), 8.35 (d, $J = 8.7$ Hz, 1H), 8.08 (dd, $J = 8.5, 3.8$ Hz, 2H), 7.96 (d, $J = 8.7$ Hz, 1H), 7.92–7.78 (m, 6H), 7.69 (t, $J = 7.5$ Hz, 1H). ^{13}C NMR (101 MHz, $CDCl_3$, δ): 137.9, 135.6, 135.4, 135.3, 134.9, 133.4, 131.9, 131.3, 131.2, 131.1, 130.8, 130.7, 129.1, 128.9, 128.85, 128.81, 128.6, 127.97, 127.94, 127.8, 127.4, 127.3, 127.1, 126.9, 126.8, 126.4, 124.6, 122.8. HRMS (MALDI-TOF) (m/z): $[M]^+$ calcd for $C_{28}H_{14}$, 350.1090; found, 350.1095.

3b. Yield: 85% (42 mg). Light yellow solid. mp 226–228 °C. 1H NMR (400 MHz, $CDCl_3$, δ): 9.28 (d, $J = 8.6$ Hz, 1H), 8.75 (d, $J = 8.9$ Hz, 1H), 8.65 (d, $J = 8.8$ Hz, 1H), 8.40 (dd, $J = 8.8, 4.7$ Hz, 2H), 8.01 (d, $J = 8.7$ Hz, 1H), 7.96–7.88 (m, 2H), 7.84 (m, 3H), 7.75 (dd, $J = 14.5, 7.5$ Hz, 1H), 7.38 (t, $J = 8.9$ Hz, 1H). ^{13}C NMR (101 MHz, $CDCl_3$, δ): 160.6, 158.1, 137.9, 135.6, 135.5 (d, $J = 2.0$ Hz), 134.8, 133.4 (d, $J = 4.0$ Hz), 131.7, 131.1, 130.9, 130.7 (d, $J = 2.7$ Hz), 128.8, 128.7, 128.5, 128.1, 128.0, 127.5, 127.4, 127.2, 126.9, 126.7, 126.6, 124.5, 124.3 (d, $J = 4.0$ Hz), 123.4, 123.2 (d, $J = 1.8$ Hz), 119.8 (d, $J = 6.9$ Hz), 110.3, 110.1. ^{19}F NMR (282 MHz, $CDCl_3$, δ): -121.48 (dd, $J = 10.0, 5.9$ Hz). HRMS (MALDI-TOF) (m/z): $[M]^+$ calcd for $C_{28}H_{13}F$, 368.1001; found, 368.1021.

3c. Yield: 91% (45 mg). Beige solid. mp 266–268 °C. 1H NMR (400 MHz, $CDCl_3$, δ): 8.96 (d, $J = 11.3$ Hz, 1H), 8.71 (d, $J = 8.9$ Hz, 1H), 8.60 (d, $J = 8.8$ Hz, 1H), 8.36 (t, $J = 9.4$ Hz, 2H), 8.01 (d, $J = 8.7$ Hz, 1H), 7.96–7.80 (m, 5H), 7.21 (t, $J = 8.3$ Hz, 1H). ^{13}C NMR (101 MHz, $CDCl_3$, δ): 162.1 (d, $J = 13.1$ Hz), 161.0 (d, $J = 13.7$ Hz), 159.7 (d, $J = 13.2$ Hz), 158.5 (d, $J = 13.6$ Hz), 137.9, 135.6, 135.5, 135.4, 134.7, 133.3 (dd, $J = 11.5, 6.6$ Hz), 132.6, 131.1, 130.9 (d, $J = 1.6$ Hz), 130.08–139.96 (m), 128.5, 128.3, 128.2, 128.0, 127.9, 127.6, 127.4, 126.9, 124.4, 122.5 (t, $J = 2.1$ Hz), 120.4 (d, $J = 1.7$ Hz), 120.2 (d, $J = 1.5$ Hz), 119.8 (dd, $J = 6.5, 1.7$ Hz), 108.7 (d, $J = 4.3$ Hz), 108.4 (d, $J = 4.4$ Hz), 101.9, 101.6 (d, $J = 4.7$ Hz), 101.4. ^{19}F NMR (373 MHz, $CDCl_3$, δ): -110.69 (dt, $J = 11.3, 8.1$ Hz), -116.70 to -116.81 (m). HRMS (MALDI-TOF) (m/z): $[M]^+$ calcd for $C_{28}H_{12}F_2$, 386.0907; found, 386.0925.

3d. Yield: 81% (41 mg). Dark yellow solid. mp 238–240 °C. 1H NMR (400 MHz, $CDCl_3$, δ): 8.76 (d, $J = 9.0$ Hz, 1H), 8.41 (t, $J = 7.2$ Hz, 1H), 8.35 (d, $J = 8.8$ Hz, 1H), 8.18 (dd, $J = 10.7, 8.9$ Hz, 1H), 8.02 (d, $J = 8.8$ Hz, 1H), 7.90–7.76 (m, $J = 15.2, 13.5, 8.9$ Hz, 5H), 7.53–7.40 (m, $J = 14.5, 12.3, 10.2$ Hz, 1H), 7.34 (td, $J = 8.8, 3.6$ Hz, 1H). ^{13}C NMR (101 MHz, $CDCl_3$, δ): 156.7, 156.3, 154.2, 153.9, 139.1, 137.9, 136.2, 135.2 (d, $J = 8.6$ Hz), 134.8, 132.7, 131.0 (d, $J = 3.8$ Hz), 130.9, 129.9 (d, $J = 2.4$ Hz), 129.6, 129.4, 128.0, 127.4 (d, $J = 3.7$ Hz), 127.1, 126.9, 126.5 (d, $J = 3.7$ Hz), 124.6, 124.1, 119.9 (dd, $J = 6.7, 2.0$ Hz), 111.9 (d, $J = 9.0$ Hz), 111.6 (d, $J = 8.9$ Hz), 110.5 (d, $J = 9.2$ Hz), 110.3 (d, $J = 9.2$ Hz). ^{19}F NMR (373 MHz, $CDCl_3$, δ): -108.40 to -108.56 (m), -125.92 to -126.05 (m). HRMS (MALDI-TOF) (m/z): $[M]^+$ calcd for $C_{28}H_{12}F_2$, 386.0907; found, 386.0919.

3e. Yield: 75% (37 mg). Beige solid. mp 298–299 °C. ¹H NMR (400 MHz, CDCl₃, δ): 8.68 (d, *J* = 8.8 Hz, 1H), 8.36 (d, *J* = 8.8 Hz, 1H), 8.17–8.09 (m, 1H), 7.99 (t, *J* = 8.7 Hz, 2H), 7.89–7.79 (m, 5H), 7.63 (dd, *J* = 16.7, 8.8 Hz, 1H). ¹³C NMR (101 MHz, CDCl₃, δ): 137.9, 136.2, 135.4, 135.2, 134.9, 131.1 (d, *J* = 1.4 Hz), 130.9, 129.5 (d, *J* = 2.3 Hz), 129.1, 128.9, 128.1, 127.5 (d, *J* = 1.0 Hz), 127.4, 127.1, 127.0, 126.8, 126.74, 126.70, 126.68, 126.66, 124.4, 124.2 (d, *J* = 2.2 Hz), 109.4 (d, *J* = 4.0 Hz), 109.3 (d, *J* = 4.1 Hz). ¹⁹F NMR (373 MHz, CDCl₃, δ): –126.82 to –127.02 (m), –134.07 to –134.33 (m), –158.83 (ddd, *J* = 20.7, 18.2, 7.4 Hz). HRMS (MALDI-TOF) (*m/z*): [M]⁺ calcd for C₂₈H₁₁F₃, 404.0813; found, 404.0817.

3f. Yield: 99% (49 mg). Beige solid. mp 205–207 °C. ¹H NMR (400 MHz, CDCl₃, δ): 9.65 (d, *J* = 8.6 Hz, 1H), 8.79 (d, *J* = 9.2 Hz, 1H), 8.53–8.43 (m, 2H), 8.35 (d, *J* = 8.8 Hz, 1H), 8.08 (d, *J* = 7.3 Hz, 1H), 7.98 (d, *J* = 8.7 Hz, 1H), 7.92–7.76 (m, 6H). ¹³C NMR (101 MHz, CDCl₃, δ): 137.8, 135.8, 135.4, 134.7, 133.0, 132.4, 131.4, 131.0 (d, *J* = 1.3 Hz), 130.8, 130.7, 129.0, 128.6, 128.4, 128.1, 128.0 (d, *J* = 3.0 Hz), 127.6, 127.3, 127.2, 127.0, 126.8, 126.6, 126.3, 124.9, 124.8 (dd, *J* = 11.9, 6.0 Hz), 124.4, 124.3, 123.6, 123.2 (q, *J* = 2.6 Hz). ¹⁹F NMR (282 MHz, CDCl₃, δ): –59.16 (s). HRMS (MALDI-TOF) (*m/z*): [M]⁺ calcd for C₂₉H₁₃F₃, 418.0963; found, 418.0943.

3g. Yield: 100% (50 mg). Beige solid. mp 223–225 °C. ¹H NMR (400 MHz, CDCl₃, δ): 8.82 (d, *J* = 9.2 Hz, 1H), 8.44–8.37 (m, 2H), 8.14–8.00 (m, 3H), 7.90–7.77 (m, 5H), 7.54 (dd, *J* = 11.8, 8.2 Hz, 1H). ¹³C NMR (101 MHz, CDCl₃, δ): 162.9, 160.4, 137.7, 136.1, 135.1, 135.0, 134.6, 132.1, 131.6 (d, *J* = 4.6 Hz), 131.0, 130.9, 130.8, 129.8 (d, *J* = 3.1 Hz), 129.2, 129.0, 128.0, 127.4, 127.1, 127.1, 127.0, 126.99, 126.91, 126.8, 126.6 (d, *J* = 3.5 Hz), 125.9 (dd, *J* = 10.6, 6.0 Hz), 125.4, 124.4, 123.3, 123.11–122.98 (m), 122.9 (d, *J* = 3.9 Hz), 122.6 (d, *J* = 3.8 Hz), 121.7, 121.6, 120.5, 110.9, 110.6. ¹⁹F NMR (282 MHz, CDCl₃, δ): –58.57 (s), –97.16 (t, *J* = 9.9 Hz). HRMS (MALDI-TOF) (*m/z*): [M]⁺ calcd for C₂₉H₁₂F₄, 436.0869; found, 436.0848.

3h. Yield: 99% (49 mg). Beige solid. mp 221–222 °C. ¹H NMR (400 MHz, CDCl₃, δ): 9.37 (dd, *J* = 10.7, 2.3 Hz, 1H), 8.78 (d, *J* = 9.2 Hz, 1H), 8.52 (d, *J* = 8.8 Hz, 1H), 8.43 (dd, *J* = 9.2, 1.6 Hz, 1H), 8.37 (d, *J* = 8.8 Hz, 1H), 8.02 (d, *J* = 8.7 Hz, 1H), 7.95 (d, *J* = 8.8 Hz, 1H), 7.93–7.82 (m, 4H), 7.80 (d, *J* = 5.6 Hz, 1H). ¹³C NMR (101 MHz, CDCl₃, δ): 160.9, 158.4, 137.9, 135.8, 135.7, 135.4 (d, *J* = 5.4 Hz), 134.6, 133.8 (d, *J* = 8.4 Hz), 131.8, 131.1, 131.0, 130.9 (d, *J* = 4.5 Hz), 130.7 (d, *J* = 4.9 Hz), 128.5, 128.2, 127.9 (d, *J* = 3.5 Hz), 127.7, 127.4, 127.0, 126.9, 126.0, 125.3, 124.3, 123.8 (d, *J* = 2.2 Hz), 123.1, 116.9, 116.8, 115.3 (d, *J* = 6.1 Hz), 115.0 (d, *J* = 6.2 Hz). ¹⁹F NMR (282 MHz, CDCl₃, δ): –59.39 (s), –113.24 – –113.43 (m). HRMS (MALDI-TOF) (*m/z*): [M]⁺ calcd for C₂₉H₁₂F₄, 436.0875; found, 436.0896.

3i. Yield: 99% (49 mg). Beige solid. mp 223–224 °C. ¹H NMR (400 MHz, CDCl₃, δ): 10.02 (s, 1H), 8.93 (d, *J* = 9.2 Hz, 1H), 8.50 (dd, *J* = 9.1, 1.6 Hz, 1H), 8.45 (d, *J* = 8.8 Hz, 1H), 8.37 (d, *J* = 8.8 Hz, 1H), 8.27 (s, 1H), 8.00 (dd, *J* = 18.2, 8.7 Hz, 2H), 7.93–7.79 (m, 4H). ¹³C NMR (101 MHz, CDCl₃, δ): 137.9, 135.8, 135.7 (d, *J* = 4.1 Hz), 135.4, 134.6, 131.9, 131.8 (d, *J* = 1.8 Hz), 131.2, 131.1, 130.9 (d, *J* = 2.5 Hz), 130.5 (dd, *J* = 9.1, 4.6 Hz), 130.4, 128.9, 128.6, 128.48–128.41 (m), 128.3, 128.3, 127.99, 127.92, 127.8, 127.7, 127.6, 127.5, 127.4, 127.3, 127.0 (d, *J* = 3.3 Hz), 126.9, 126.8, 125.9, 124.2, 122.9 (d, *J* = 2.8 Hz), 120.70, 120.68, 120.65. ¹⁹F NMR (282 MHz, CDCl₃, δ): –59.62 (s), –62.21 (s). HRMS (MALDI-TOF) (*m/z*): [M]⁺ calcd for C₃₀H₁₂F₆, 486.0837; found, 486.0823.

3j. Yield: 99% (49 mg). Light yellow solid. mp 207–208 °C. ¹H NMR (400 MHz, CDCl₃, δ): 8.76 (d, *J* = 9.1 Hz, 1H), 8.43–8.33 (m, 2H), 8.24 (d, *J* = 7.8 Hz, 1H), 8.17 (d, *J* = 7.8 Hz, 1H), 8.00 (d, *J* = 8.8 Hz, 2H), 7.88–7.73 (m, 4H), 7.47–7.32 (m, 1H). ¹³C NMR (101 MHz, CDCl₃, δ): 137.9, 137.2, 135.8, 135.6, 135.3, 133.4, 133.3, 133.0, 132.3, 131.79, 131.76, 131.74, 131.72, 131.3, 131.1, 130.8, 130.6, 129.9, 129.6, 129.4, 128.9, 128.6, 128.3, 127.9, 127.5 (d, *J* = 3.4 Hz), 127.3, 127.2 (d, *J* = 3.4 Hz), 127.0 (d, *J* = 2.4 Hz), 126.9 (d, *J* = 4.8 Hz), 125.9, 125.5, 125.3, 125.0, 123.8 (q, *J* = 6.1 Hz), 123.2, 122.7 (dd, *J* = 5.2, 2.4 Hz). ¹⁹F NMR (282 MHz, CDCl₃, δ): –50.11 (s), –59.17 (s). HRMS (MALDI-TOF) (*m/z*): [M]⁺ calcd for C₃₀H₁₂F₆, 486.0843; found, 486.0836.

Computational Methods. Geometry optimizations were performed for corannulene and its derivatives (3a–j) using DFT as implemented in the Amsterdam density functional (ADF) program^{20,21} with the B3LYP functional and the all-electron triple- ζ double polarization (TZ2P) basis set.^{22,23} In the process of optimization, vibrational frequency calculations confirmed no imaginary frequencies for each of the optimized molecules, which indicates that the optimized structures are at the minima of the potential energy surface.

■ ASSOCIATED CONTENT

Supporting Information

The Supporting Information is available free of charge on the ACS Publications website at DOI: 10.1021/acs.joc.7b03146.

NMR spectra of products (PDF)

Large scale syntheses procedures, optical and CV characterization, and DFT-calculations details (PDF)

■ AUTHOR INFORMATION

Corresponding Authors

*E-mail: junehuh@korea.ac.kr

*E-mail: mstuparu@ntu.edu.sg

ORCID

Mihaiela C. Stuparu: 0000-0001-8663-6189

Notes

The authors declare no competing financial interest.

■ ACKNOWLEDGMENTS

M.C.S. wishes to thank NTU Singapore (M4081566) for financial support. J.H. acknowledges support from NRF-Korea (NRF-2016R1A6A3A11933393).

■ REFERENCES

- (1) Kuvychko, I. V.; Spisak, S. N.; Chen, Y.-S.; Popov, A. A.; Petrukhina, M. A.; Strauss, S. H.; Boltalina, O. V. *Angew. Chem., Int. Ed.* **2012**, *51* (20), 4939–4942.
- (2) Schmidt, B. M.; Seki, S.; Topolinski, B.; Ohkubo, K.; Fukuzumi, S.; Sakurai, H.; Lentz, D. *Angew. Chem., Int. Ed.* **2012**, *51* (45), 11385–11388.
- (3) Kuvychko, I. V.; Dubceac, C.; Deng, S. H. M.; Wang, X.-B.; Granovsky, A. A.; Popov, A. A.; Petrukhina, M. A.; Strauss, S. H.; Boltalina, O. V. *Angew. Chem., Int. Ed.* **2013**, *52* (29), 7505–7508.
- (4) Schmidt, B. M.; Topolinski, B.; Yamada, M.; Higashibayashi, S.; Shionoya, M.; Sakurai, H.; Lentz, D. *Chem. - Eur. J.* **2013**, *19* (41), 13872–13880.
- (5) Xia, Y.; Guo, T.; Baldrige, K. K.; Siegel, J. S. *Eur. J. Org. Chem.* **2017**, *2017* (4), 875–879.
- (6) Schmidt, B. M.; Lentz, D. *Chem. Lett.* **2014**, *43* (2), 171–177.
- (7) Dutta, A. K.; Linden, A.; Zoppi, L.; Baldrige, K. K.; Siegel, J. S. *Angew. Chem., Int. Ed.* **2015**, *54* (37), 10792–10796.
- (8) Rajeshkumar, V.; Stuparu, M. C. *Chem. Commun.* **2016**, *52*, 9957–9960.
- (9) Sygula, A.; Sygula, R.; Rabideau, P. W. *Org. Lett.* **2006**, *8* (25), 5909–5911.
- (10) Rajeshkumar, V.; Courté, M.; Fichou, D.; Stuparu, M. C. *Eur. J. Org. Chem.* **2016**, *2016* (36), 6010–6014.
- (11) Boedigheimer, H.; Ferrence, G. M.; Lash, T. D. *J. Org. Chem.* **2010**, *75* (8), 2518–2527.
- (12) Ota, K.; Tanaka, T.; Osuka, A. *Org. Lett.* **2014**, *16* (11), 2974–2977.
- (13) Li, J.; Terec, A.; Wang, Y.; Joshi, H.; Lu, Y.; Sun, H.; Stuparu, M. C. *J. Am. Chem. Soc.* **2017**, *139* (8), 3089–3094.
- (14) Rajeshkumar, V.; Lee, Y. T.; Stuparu, M. C. *Eur. J. Org. Chem.* **2016**, *2016* (1), 36–40.
- (15) Wittig, G.; Schöllkopf, U. *Chem. Ber.* **1954**, *87* (9), 1318–1330.

- (16) Wittig, G.; Haag, W. *Chem. Ber.* **1955**, *88* (11), 1654–1666.
- (17) Scholz, M.; Mühlstädt, M.; Dietz, F. *Tetrahedron Lett.* **1967**, *8* (7), 665–668.
- (18) Flammang-Barbieux, M.; Nasielski, J.; Martin, R. H. *Tetrahedron Lett.* **1967**, *8*, 743–744.
- (19) Kissinger, P.; Heineman, W. R. *Laboratory Techniques in Electroanalytical Chemistry*, Second ed.; CRC Press, 1996.
- (20) te Velde, G.; Bickelhaupt, F. M.; Baerends, E. J.; Guerra, C. F.; Van Gisbergen, S.; Snijders, J. G.; Ziegler, T. J. *Comput. Chem.* **2001**, *22* (9), 931–967.
- (21) Guerra, C. F.; Snijders, J. G.; te Velde, G.; Baerends, E. J. *Theor. Chem. Acc.* **1998**, *99* (6), 391–403.
- (22) Becke, A. D. *J. Chem. Phys.* **1993**, *98* (7), 5648–5652.
- (23) Van Lenthe, E.; Baerends, E. J. *J. Comput. Chem.* **2003**, *24* (9), 1142–1156.